

Low-Thrust Maneuvers for the Efficient Correction of Orbital Elements

IEPC-2011-102

*Presented at the 32nd International Electric Propulsion Conference,
Wiesbaden • Germany
September 11 – 15, 2011*

A. Ruggiero¹ P. Pergola²
Alta, Pisa, 56100, Italy

S. Marcuccio³ and M. Andrenucci⁴
University of Pisa, Pisa, 56100, Italy

In this study, low-thrust strategies aimed at the modification of specific orbital elements are investigated and presented. Closed loop guidance laws, steering the initial value of a given orbital element to a target value, are derived, implemented and tested. The thrust laws have been defined analyzing the Gauss form of the Lagrange Planetary Equations isolating the relevant contributions to change specific orbital elements. In particular, considering the classical two body dynamics with the inclusion of the thrust acceleration, both optimal and near-optimal thrusting strategies have been obtained. In the study these thrust laws are described and special focus is given both to the thrusting time and to the total velocity increment required to perform specific or combined orbital parameter changes. The results, obtained by direct numerical simulations of the presented control laws, are compared with analytical approximation and, as study cases, some low-thrust transfers are also simulated. A direct transfer between the standard geosynchronous transfer orbit and the geosynchronous orbit is implemented together with generic demonstrations of the single strategies.

Nomenclature

a	=	semi-major axis
e	=	eccentricity
i	=	inclination
Ω	=	right ascension of the ascending node
v	=	true anomaly
E	=	eccentric anomaly
ω	=	argument of perigee
t	=	time
ΔV	=	velocity increment
\vec{f}	=	spacecraft acceleration
α	=	in-plane thrust angle

¹ Research Engineer, Alta, Pisa; M.Sc.; a.ruggiero@alta-space.com.

² Project Manager, Alta, Pisa; Ph.D.; p.pergola@alta-space.com.

³ Professor, Department of Aerospace Engineering, University of Pisa; Vice President, Alta, Pisa; s.marcuccio@alta-space.com

⁴ Professor, Department of Aerospace Engineering, University of Pisa; CEO, Alta, Pisa; m.andrenucci@alta-space.com.

β	=	out-of-plane thrust angle
η	=	maneuver efficiency
h	=	orbit angular momentum
μ	=	Earth's gravitational parameter

I. Introduction

THE use of Electric Propulsion (EP) as main propulsion system typically increases the payload mass fraction with respect to the case of chemical propulsion, reducing the propellant required to perform given orbital maneuvers. Electric thrusters have been used for missions involving orbit-to-body transfers^{1,2} as well as for orbit insertion maneuvers of satellites in geocentric trajectories³ proving their reliability and effectiveness in high total impulse missions. Together with a high exhaust velocity, EP provides low acceleration levels resulting in long transfer times during which the thruster is operated and the thrusting direction has to be controlled. The design of optimal transfer trajectories is a challenging task, even more difficult if hundreds or thousands orbital revolutions (like in the near-Earth region) and intermediate costing arcs are required⁴.

Many different methods have been used so far to design tailored trajectories for specific missions⁵ or for the exploitation of particular space regions of potential commercial interest⁶. The shooting method for the solution of the two-point boundary value problem, as well as direct collocation methods involving a huge number of nodes⁷, are widely used to determine the transfer problem by nonlinear programming and averaging techniques.

In Sec. II of this study, the problem of the low-thrust transfer from an initial orbit to a target one is addressed by investigating the analytical expressions of the instantaneous variation of the Classical Orbital Elements (COEs) in a two body model perturbed by the thruster action. These variations are modeled by means of the well-known Lagrange Planetary Equations (LPE)⁸. In particular, the acceleration exerted by the thruster accounts as the only perturbation acting on the spacecraft and any other perturbative effect is neglected. Moreover, since we are not investigating rendezvous maneuver, the true anomaly instantaneous rate of change equation is ignored and only five LPE, in their Gauss form⁸, are considered. Some examples and test cases for each COE variation are provided at the end of Sec. II.

For each COE change, the ratio between the optimal instantaneous change and the maximum allowable one over the orbit are derived and used to cut off thrusting when below a given threshold. This latter ratio, derived in Sec. III for each COE, represents a sort of efficiency factor for the element change and allows to activate or deactivate a specific thrusting strategy.

The strategy to change at the same time more than a single orbital element is derived, in Sec. IV, as the weighted sum of different strategies, considering during the whole transfers the difference between osculating and target COEs as weight for the optimal thrusting vector.

Finally, the obtained guidance schemes have been verified by means of direct integrations. During the integration, the mass is considered as variable and the resulting mass consumption is used to estimate, by means of the Tsiolkovsky's rocket equation⁹, the velocity increment corresponding to the performed maneuver. The obtained velocity increment values are also compared with the available analytical expressions for optimum low-thrust transfers. The mass consumption and the time required to perform the desired maneuver are also assessed for discontinuous thrusting transfers, for various thresholds of the COE change efficiency factor.

All the orbital computation carried out in this study have been performed using Alta in-house developed orbital propagator SATSLab^{10,11}.

II. Thrusting Laws for Classical Orbital Elements Correction

The identification of the relation between an external perturbation and rate of change of COEs represents a key point for the definition and design of specific steering programs. The time rates of change of the relevant five parameters are given by the Gauss form of the LPE⁸:

$$\begin{aligned}
\frac{da}{dt} &= \frac{2a^2}{h} \left\{ e f_R \sin \nu + \frac{p}{r} f_C \right\} \\
\frac{de}{dt} &= \frac{1}{h} \left\{ p f_R \sin \nu + f_C \left((p+r) \cos \nu + r e \right) \right\} \\
\frac{di}{dt} &= \frac{r \cos \mathcal{G}}{h} f_N \\
\frac{d\Omega}{dt} &= \frac{r \sin \mathcal{G}}{h \sin i} f_N \\
\frac{d\omega}{dt} &= \frac{1}{h e} \left\{ -p f_R \cos \nu + (p+r) f_C \sin \nu \right\} - \frac{r \sin \mathcal{G}}{h \sin i} f_N \cos i
\end{aligned} \tag{1}$$

where p is the semilatus rectum, \mathcal{G} is given by the sum of argument of perigee (ω) and true anomaly (ν), h is orbit angular momentum and μ represents Earth's gravitational parameter ($\sim 398600 \text{ km}^3\text{s}^{-2}$). Moreover, in Eq. 1, the acceleration exerted by the thruster on the spacecraft (\vec{f}) is expressed by its components in the body-fixed radial-circumferential-normal (RCN) reference frame (f_R, f_C, f_N)⁹. This reference is such that the radial component is aligned with the radial unit vector positive in the Zenith direction, the normal component is aligned with the osculating angular momentum vector positive in the direction of the cross product $\vec{R} \times \vec{V}$ and the circumferential component is normal to the radius vector in the orbital plane and completes the left-handed triad of unit vectors (see Fig. 1 left).

It is interesting to note that the last term of the fifth equation of Eqs. 1 can be interpreted as the instantaneous variation of the right ascension of the ascending node times the cosine of the orbital inclination.

Introducing the in-plane ($-\pi < \alpha < \pi$, positive, starting from the circumferential direction away from the central body) and of the out-of-plane ($-\pi/2 < \beta < \pi/2$, positive, starting from orbital plane, in the direction of the angular momentum) thrust angles (see Fig. 1 right), the acceleration components can be expressed as:

$$\begin{aligned}
f_R &= |\vec{f}| \cos \beta \sin \alpha \\
f_C &= |\vec{f}| \cos \beta \cos \alpha \\
f_N &= |\vec{f}| \sin \beta
\end{aligned} \tag{2}$$

The direct substitution of the expressions of Eq. 2 in the Gauss form of the LPE (Eqs. 1) gives:

$$\begin{aligned}
\frac{da}{dt} &= \frac{2a^2}{h} |\vec{f}| \cos \beta \left\{ e \sin \nu \sin \alpha + \frac{p}{r} \cos \alpha \right\} \\
\frac{de}{dt} &= \frac{1}{h} |\vec{f}| \cos \beta \left\{ p \sin \nu \sin \alpha + \left((p+r) \cos \nu + r e \right) \cos \alpha \right\} \\
\frac{di}{dt} &= |\vec{f}| \frac{r}{h} \cos \mathcal{G} \sin \beta \\
\frac{d\Omega}{dt} &= |\vec{f}| \frac{r \sin \mathcal{G}}{h \sin i} \sin \beta \\
\frac{d\omega}{dt} &= \frac{1}{h e} |\vec{f}| \cos \beta \left\{ -p \cos \nu \sin \alpha + (p+r) \sin \nu \cos \alpha \right\} - \frac{r \sin \mathcal{G} \cos i}{h \sin i} \sin \beta
\end{aligned} \tag{3}$$

Equations 3 represent, for each orbital element, an analytical relation between thrust angles (α, β) and the instantaneous variation of each orbital element.

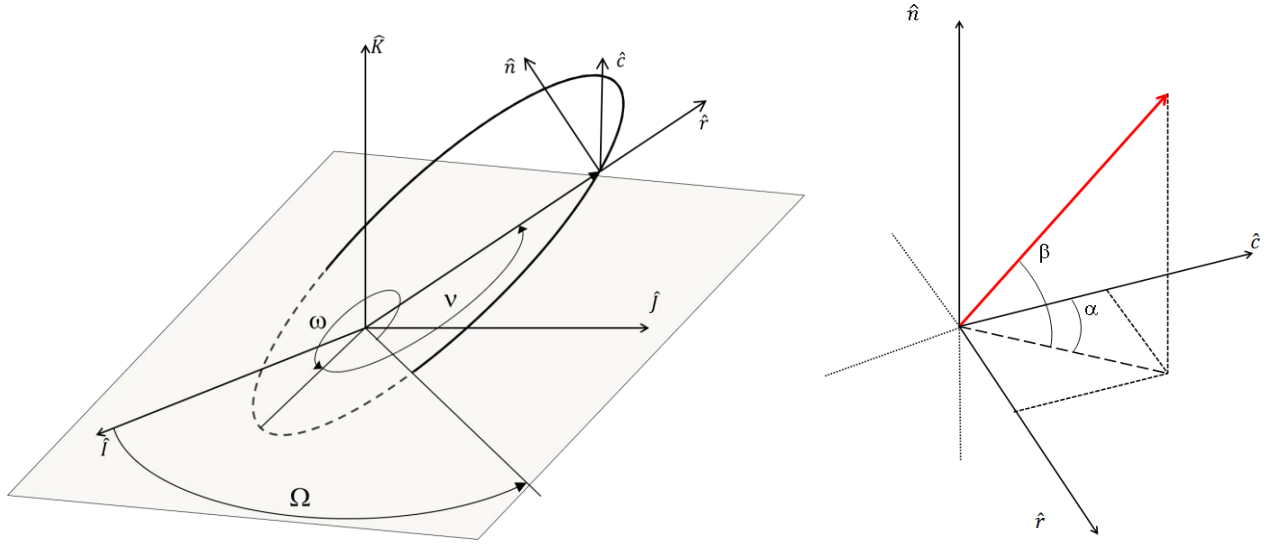


Figure 1. Left: RCN reference frame with respect to the Earth-Centered inertial reference frame (IJK). Right: α and β thrust angles with respect to the RCN reference frame.

A. Optimal and quasi-optimal thrusting laws

The first partial derivatives of Eqs. 3 with respect to thrust angles allow identifying the thrust angle value providing the highest instantaneous COEs rate of change as a function of true anomaly. In particular, considering the derivative of the first and second of Eqs. 3 with respect to the out-of-plane thrust angle (β), we get the well-known result that the rate of change of semi-major axis and eccentricity is maximum for $\beta = 0$, i.e. for planar thrusting¹². Under this assumption, taking the first order derivative of the first and second of Eqs. 3 with respect to the in-plane thrust angle (α), we can identify the optimal α angle as a function of orbital position (see Tab. 1); as expected, the thrust angle enabling the maximum semi-major axis rate of change is equal to the instantaneous flight path angle, i.e. the thrusting vector must be always aligned with the velocity vector¹².

Similarly, it is possible to notice that inclination and RAAN are only dependent on the out-of-plane thrust angle and their rate of change are at their maximum for $\beta = \pi/2$ ($di/dt > 0$, $d\Omega/dt > 0$) or $\beta = -\pi/2$ ($di/dt < 0$, $d\Omega/dt < 0$), i.e. for thrust always normal to the instantaneous orbital plane. Accordingly, their instantaneous rate of change does not depend from the in-plane thrust angle (α). In particular, inclination can be changed thrusting along the angular momentum vector and changing the thrusting direction according to the out-of-plane velocity component sign, to rotate the velocity vector cumulating the thrusting effect over each orbit. Similarly, the RAAN can be modified thrusting along the angular momentum and changing direction according to the sign of the scalar product of the velocity with the line of nodes.

An instantaneous variation of the argument of perigee can always be obtained keeping at least one of the two thrust angles non-identically zero. In the more general case ($\alpha \neq 0$, $\beta \neq 0$), two different laws can be identified for the in-plane and out-of-plane thrust angles providing the maximum argument of perigee rate of change. It is worth mentioning again that the rates of change of argument of perigee and RAAN are closely related: in particular, a thrust vector with an out-of-plane thrust angle causes an instantaneous net change both of argument of perigee and RAAN.

Table 1 shows, for each COE, the in-plane and out-of-plane thrust angles providing the highest instantaneous COE rate of change computed with the approach sketched above.

	Thrusting angles	
Semi-major axis (a)	$\alpha = \arctan\left(\frac{e \sin \nu}{1 + e \cos \nu}\right)$	$\beta = 0$ (4)
Eccentricity (e)	$\alpha = \arctan\left(\frac{\sin \nu}{\cos \nu + \cos E}\right)$	$\beta = 0$ (5)
Inclination (i)	$\alpha = 0$	$\beta = \operatorname{sgn}(\cos(\omega + \nu)) \cdot \frac{\pi}{2}$ (6)
RAAN (Ω)	$\alpha = 0$	$\beta = \operatorname{sgn}(\sin(\omega + \nu)) \cdot \frac{\pi}{2}$ (7)
Argument of Perigee (ω)	$\alpha = \arctan\left(\frac{1 + e \cos \nu}{2 + e \cos \nu} \cot \nu\right)$ $\beta = \arctan\left(\frac{e \cot i \sin(\omega + \nu)}{\sin(\alpha - \nu)(1 + e \cos \nu) - \cos(\alpha) \sin \nu}\right)$ (8)	

Table 1. Optimal in-plane (α) and out-of-plane (β) thrust angles for the maximum instantaneous change of each orbital element.

It is worth mentioning that also some simplified thrusting strategies aimed at obtaining pure changes of semi-major axis, eccentricity or argument of perigee are available in literature¹³⁻¹⁵. These are here summarized for convenience and to compare the results obtained in Sec. II.B with these reference values.

The argument of perigee can be modified, without any effect on semi-major axis and eccentricity, thrusting in the direction of orbit eccentricity vector (i.e. along semi-major axis)¹⁶. The velocity increment (ΔV) required to obtain a given change ($\Delta \omega$) is given by¹⁶:

$$\Delta V = \sqrt{\frac{\mu}{a}} \frac{2}{3} \frac{e}{\sqrt{1-e^2}} |\Delta \omega| \quad (9)$$

Moreover, this thrusting scheme is a quite uncommon example of low-thrust maneuver whose ΔV is smaller (66.7%) than the one of the corresponding impulsive case¹⁶.

Orbital eccentricity can be modified thrusting orthogonally to orbit eccentricity vector¹²⁻¹⁴. Equation 10 shows the total velocity increment required to realize a net eccentricity change from an initial value (e_1) to a final value (e_2):

$$\Delta V = \sqrt{\frac{\mu}{a}} \frac{2}{3} |\arcsin(e_1) - \arcsin(e_2)| \quad (10)$$

This thrusting strategy provides, for quasi-circular orbits, results very close to the optimal ones¹². In particular, this steering program requires a velocity increment less than 3% larger than the optimum one¹⁴. More in general, a net eccentricity change with a null semi-major axis variation can be obtained exerting a constant radial acceleration over the orbit and a circumferential acceleration component reversed when the eccentric anomaly $E = \pm \pi/2$. Similarly, the semi-major axis can be altered, with no change in orbit eccentricity, perturbing the orbit with a constant circumferential acceleration and a radial acceleration reversed in sign when $E = 0$ or π ¹⁷.

For the sake of completeness, Tab. 2 shows also the velocity increment required, for quasi-circular orbit, to obtain a change in orbit RAAN, semi-major axis or inclination.

	Semi-major axis (a)	Inclination (i)	RAAN (Ω)
ΔV	$\Delta V = \left \sqrt{\frac{\mu}{a_0}} - \sqrt{\frac{\mu}{a_1}} \right $ (11) Ref.10	$\Delta V = V \sqrt{2 - 2 \cos \frac{\pi}{2} \Delta i}$ (12) Ref.10	$\Delta V = \frac{\pi}{2} \sqrt{\frac{\mu}{a}} \Delta \Omega \sin(i)$ (13) Ref.12

Table 2. Expressions of the velocity increment required to obtain a change in orbit RAAN, semi-major axis or inclination.

In the first two expressions of Tab. 2, derived by Edelbaum¹² under the assumption of constant spacecraft acceleration, a_0 and a_1 represent initial and final orbit semi-major axis and Δi represents the desired inclination change. In the last equation of Tab. 2 derived by Pollard¹⁴, $\Delta\Omega$ is the desired RAAN change.

B. Test Cases

Some examples of orbital maneuver aimed at the modification of a single COE are presented in this section considering a small satellite equipped with an electric propulsion system. In particular, the spacecraft is envisaged to have an initial mass of 367 kg (the same of SMART-1 at the beginning of his life¹⁸) and a Snecma PPS-1350 Hall Effect Thruster (HET) (again the same thruster operating at lower power level in the SMART-1 mission¹⁸). The relevant spacecraft and thruster characteristics are summarized in Tab. 3.

The EP is operated also during eclipse phases and no other orbital perturbations are considered, apart from the one produced by the thruster. In each case a different set of initial and final COEs, significant for the case under investigation, is assumed.

Initial Mass	367 kg
Thruster	Snecma PPS [®] 1350
Power	1.5 kW
Thrust	89 mN (Ref.17)
Specific Impulse	1650 s (Ref.17)
Initial Acceleration	$2.4e-4 \text{ m}\cdot\text{s}^{-2}$

Table 3. Relevant spacecraft and thruster characteristics.

The steering program described by Eq. 4 is used to increase the semi-major axis of a circular orbit from an altitude of 1000 km up to the Geosynchronous Earth Orbit (GEO); results are presented in Fig. 2.

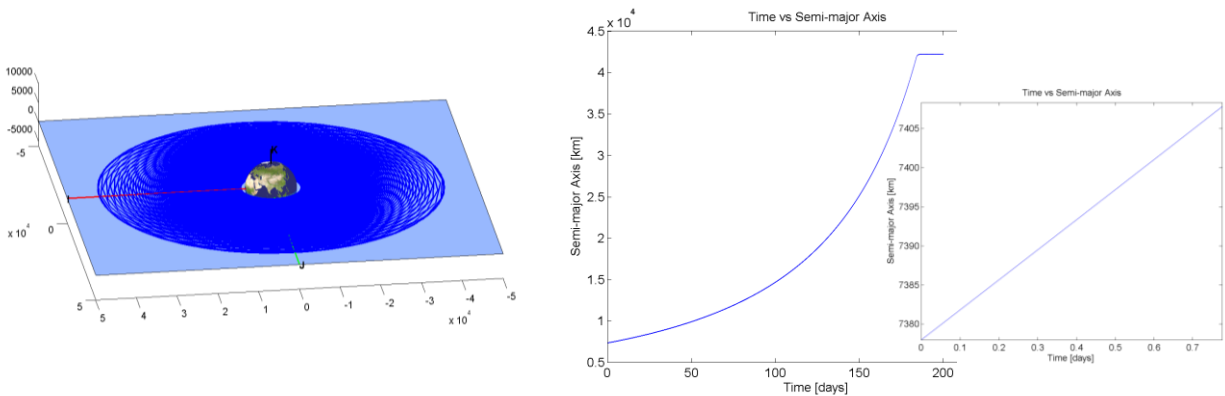


Figure 2. Spacecraft trajectory (left) and time evolution of orbit semi-major axis with a close up of the evolution over one orbit (right).

Figure 2 shows spacecraft trajectory from Low Earth Orbit (LEO) to GEO (left) and semi-major axis growth during the whole maneuver (right) and over a single orbit (in the close-up). About 87.5 kg of propellant and 186 days are required to perform the considered maneuver. Tsiolkovsky's rocket equation⁹ can be used to assess the velocity increment required (4.4 km/s). This value differs by 3% from the one predicted by Eq.11 (4.27 km/s) due to the constant acceleration assumption of this latter expression.

The thrusting strategy described in Eq. 5 is used to increase the eccentricity of a circular orbit. Considering a 900 km Sun-synchronous orbit, an increase of orbital eccentricity can eventually result in the spacecraft disposal, so an Earth impact trajectory is considered as target orbit. Figure 3 shows spacecraft trajectory (left) and the time evolution of orbit eccentricity (right) again over the whole simulation and over a single orbit. The small oscillations that can be observed in the close-up are due the non-uniform efficiency of the maneuver (see Sec. III).

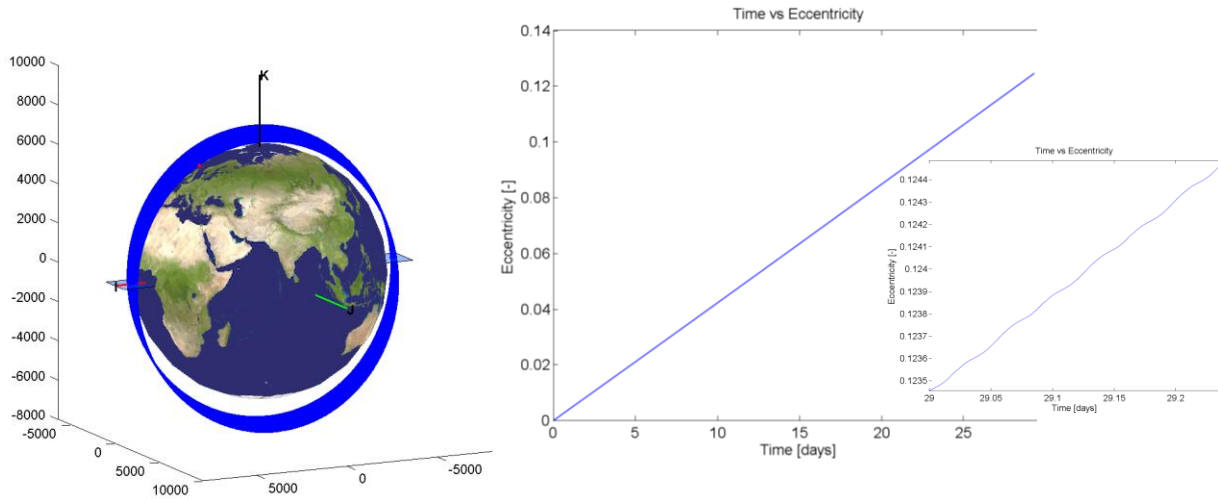


Figure 3. Spacecraft trajectory (left), the red dot highlights the impact point. The right plot shows the time evolution of orbit eccentricity and a close up of the evolution over one orbit.

About 14 kg of propellant and one month are sufficient to deorbit the spacecraft from the initial circular orbit. The velocity increment required is about 615.8 m/s and is close to the one predicted by Eq. 10 (615.84 m/s).

As representative pure inclination change, a transfer from 46 deg (Baikonur Cosmodrome latitude) to 51.6 deg for a circular ISS-like orbit (~350 km of altitude) is addressed. The thrust law considered is the one of Eq. 6 and results are presented in Fig. 4:

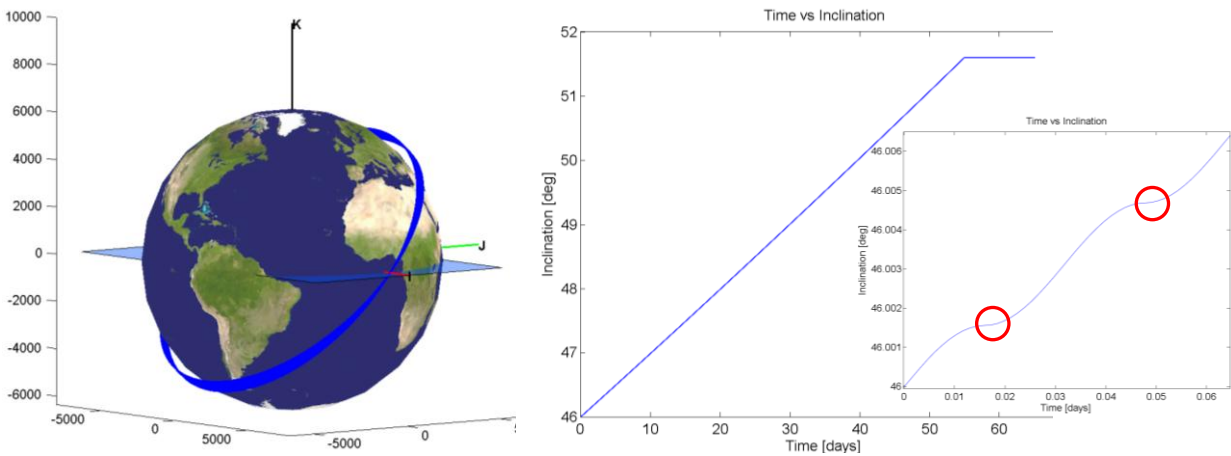


Figure 4. Orbit trajectory (left) and the orbital inclination evolution in time (right). In the close-up, the inclination change in a single orbit and, in the red circles, two inclination change plateaus.

The left plot of Fig. 4 shows the orbit trajectory and the right one shows orbital inclination evolution in time and a close-up over a single orbit. It is easy to notice the different efficacy of the thrusting strategy used over the orbit. Two different parts of the plot, highlighted by red circles, represent arcs of the orbit during which thruster operation does not produce an appreciable inclination change. The propellant required to perform the considered inclination change is 25.8 kg and the total maneuver time results to be smaller than 54 days. The required ΔV , compliant with the one predicted by Eq. 12, is about 1.18 km/s.

An arbitrary change of 5 deg of orbit RAAN, performed by means of the steering law described by Eq. 7, for a 900 km Sun-synchronous orbit is here considered. In Fig. 5, the left plot shows spacecraft trajectory while the right one the RAAN time evolution with a close-up of its changing over a single orbit.

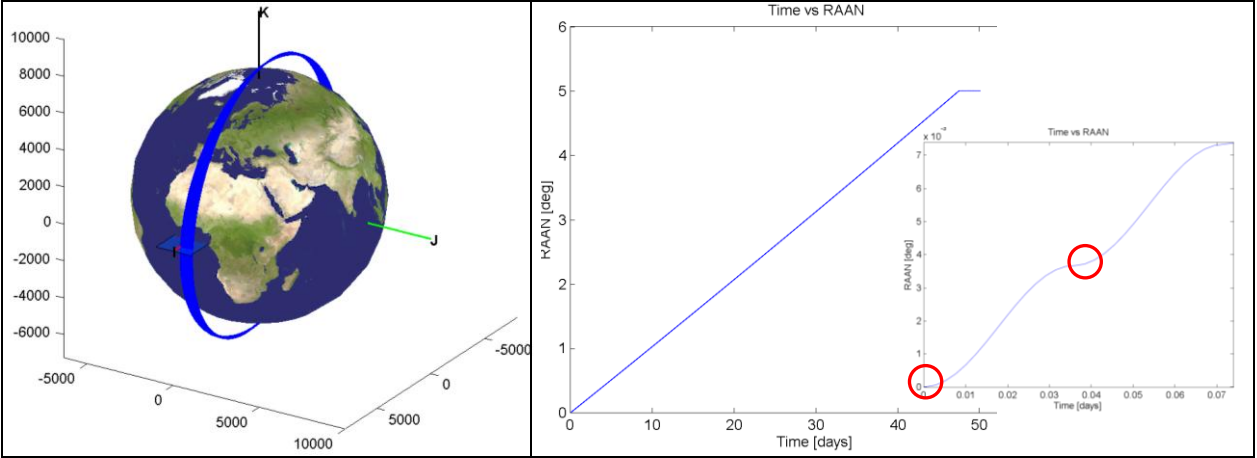


Figure 5. Orbit trajectory (left) and RAAN evolution in time (right). In the close-up, the RAAN increase in a single orbit and, in the red circles, two arc where thrust does not produce an appreciable RAAN changing.

About 48 days and 23.5 kg of propellant are sufficient to obtain the desired RAAN change with a corresponding velocity increment of about 1070 m/s. Similarly to the case of inclination change, two arc of the orbit (red circles) during which thruster operation does not produce an appreciable RAAN change can be noticed.

A Soyuz standard GTO is assumed as initial orbit and an argument of perigee change of 5 deg is performed exploiting the steering program described by Eq. 8. Figure 6 shows spacecraft trajectory (left) and the time evolution of orbit argument of perigee (right) with a close-up of the change over a single orbit.

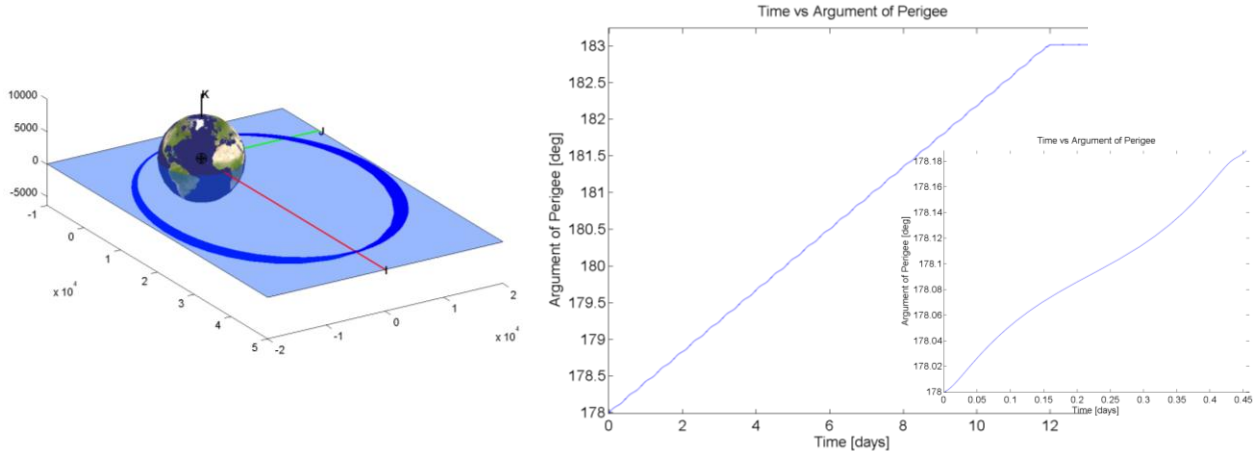


Figure 6. Orbit trajectory (left) and changing in time of the argument of perigee (right). In the close-up, the increase of argument of perigee in a single orbit.

The desired argument of perigee changing can be achieved in about 12 days using less than 6 kg of propellant. The corresponding velocity increment is about 248.9 m/s while the one predicted by means of Eq. 9 is 249.9 m/s.

III. Maneuver Efficiency

Every COE change described in Sec. II, as it can be noticed in close-ups of Fig. 2 - 6, exhibits a non-uniform magnitude variation along the path from initial to final orbit. As a matter of fact, in one or more points of the orbit the COEs growth is at a minimum or even zero. Thus, by setting the first order derivative of Eqs. 3 with respect to true anomaly equal to zero, it is possible to identify the points of the orbit enabling a maximum (v_{max}), minimum or null COE change and the corresponding variation.

Based on such a kind of analysis, it is then possible to distinguish those arcs of the orbit where thrust does not produce big effects and where coasting may represent, in terms of mass consumption, a more effective choice. In

particular, the ratio between the instantaneous rate of change of a specific COE and the maximum obtainable COE variation, considering the osculating orbital elements, has been defined as maneuver efficiency, η_{COE} :

$$\eta_{\text{COE}} = \frac{d\text{COE}/dt}{d\text{COE}/dt|_{v_{\text{max}}}} \quad (14)$$

It is worth stressing that a unique choice for the length of the coasting arcs does not exist and the definition of an efficiency threshold results in a COE changing only during some arcs and ballistic phases otherwise. Such a threshold ($\eta > \eta_{\text{Th}}$) might cause longer maneuver time, but a smaller propellant mass consumption for a given COE if compared with the continuous thrusting strategy variation. The point of the orbit providing the maximum rate of change and the expression of η , obtained by means of the described approach, used also in Ref. 15 and Ref. 20-22, for each COE are listed in Tab. 4.

COE	v_{max}	η
a	$v_a = 0$	$\eta_a = \vec{v} \sqrt{\frac{a}{\mu} \frac{1-e}{1+e}}$
e	$v_e = \pi$	$\eta_e = 2 \frac{1+2e \cos v + \cos^2 v}{1+e \cos v}$
i	$\sin(v_i + \omega) = -e \sin \omega$	$\eta_i = \frac{ \cos(\omega + v) }{1+e \cos v} \left(\sqrt{1-e^2 \sin^2 \omega} - e \cos \omega \right)$
Ω	$\cos(v_\Omega + \omega) = -e \cos \omega$	$\eta_\Omega = \frac{ \sin(\omega + v) }{1+e \cos v} \left(\sqrt{1-e^2 \cos^2 \omega} - e \sin \omega \right)$
ω	$\cos v_\omega = \left[\frac{1-e^2}{e^3} + \sqrt{\frac{1}{4} \left(\frac{1-e^2}{e^3} \right)^2 + \frac{1}{27}} \right]^{\frac{1}{3}} - \left[-\frac{1-e^2}{e^3} + \sqrt{\frac{1}{4} \left(\frac{1-e^2}{e^3} \right)^2 + \frac{1}{27}} \right]^{\frac{1}{3}} - \frac{1}{e}$	$\eta_\omega = \frac{1 + \sin^2 v}{1 + e \cos v} \frac{1 + e \cos v_{\omega \text{max}}}{1 + \sin^2 v_{\omega \text{max}}}$

Table 4. Point of the orbit providing the maximum rate of change and the expression of the maneuver efficiency, η , for each considered COE.

By way of example, the inclination change represented in Fig. 4 has been computed again assuming different maneuver efficiency thresholds. Figure 7 shows the total maneuver time and the propellant mass consumption for each efficiency value (left) and the thrusting arcs (in red) with the thrust directions for the trajectory corresponding to an efficiency value of 50%. In this case, the required inclination change of 5.6 deg can be realized in 64 days and with 20 kg of propellant.

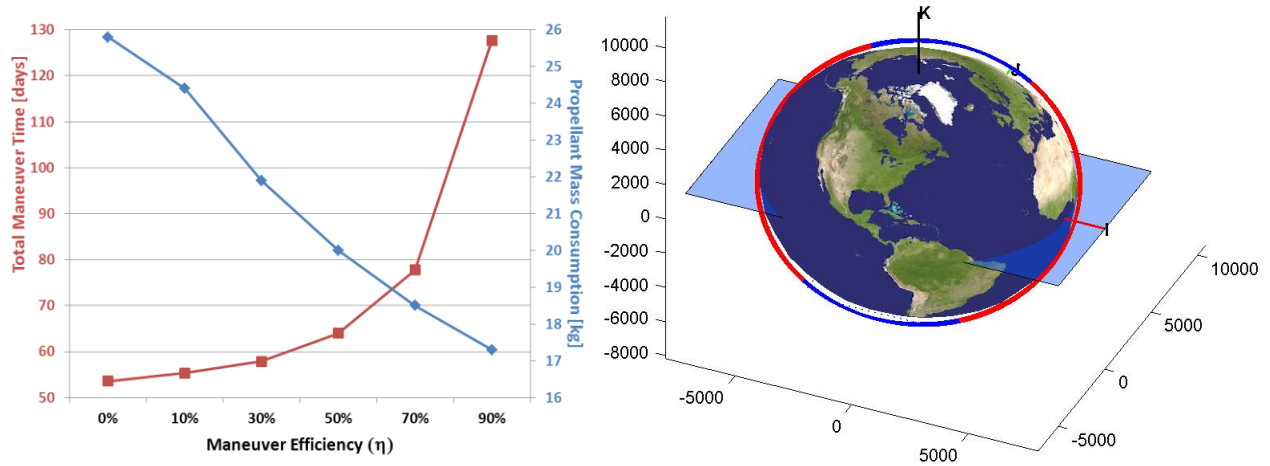


Figure 7. Left: maneuver time (red line) and propellant mass consumption (blue line) for each efficiency value. Right: Orbit with thrusting arcs (in red) for an efficiency value of 50%.

IV. Combined Classical Orbital Elements Correction

In the more general case of initial and final orbit differing for more than one single COE, the most suitable spacecraft trajectory would be the one modifying at the same time all the required COEs. This steering program is here simply implemented considering the ratio between the osculating value of the specific COE and the target one for the same COE at each time step. These ratios have been used as weights to obtain the final thrusting vector direction. Mathematically, the thrusting vector can be obtained by means of:

$$\vec{T} = \sum_{\text{COE}} \left(1 - \delta_{\text{COE}, \text{COE}_1}\right) \frac{\text{COE}_1 - \text{COE}}{\text{COE}_1 - \text{COE}_0} \vec{T}_{\text{COE}} \quad (15)$$

where COE, COE₁ and COE₀ represent respectively instantaneous osculating, target and initial value of a specific orbital element, \vec{T}_{COE} is the instantaneous direction of the optimal thrusting vector for the modification of the COE and $\delta_{\text{COE}, \text{COE}_1}$ is the Kronecker delta. In this way these self-adaptive weights assure the completion of all maneuvers at the same time and imply a thrust direction changing according with the larger COE error at a given instant.

A. Test Cases

A relevant example of orbital maneuver requiring the combined modification of more than one COE is the transfer from a GTO to a GEO orbit. Soyuz standard GTO (see Fig. 6) has been assumed as initial orbit and three out of five orbital elements (a , e , i) are modified by the steering program. A spacecraft with the characteristics listed in Tab. 3 has been assumed also in this case. Table 5 shows the targeted values of semi-major axis, eccentricity and inclination.

COE	Initial Orbit	Target Orbit
a	24396 km	42164 km
e	0.7283	0
i	7 deg	0 deg

Table 5. Initial and target values for the COEs considered.

The transfer trajectory (see Fig. 8), obtained by means of the steering program described by Eq. 15, allows to achieve target orbit conditions in 103.9 days with a propellant mass consumption of 49 kg.

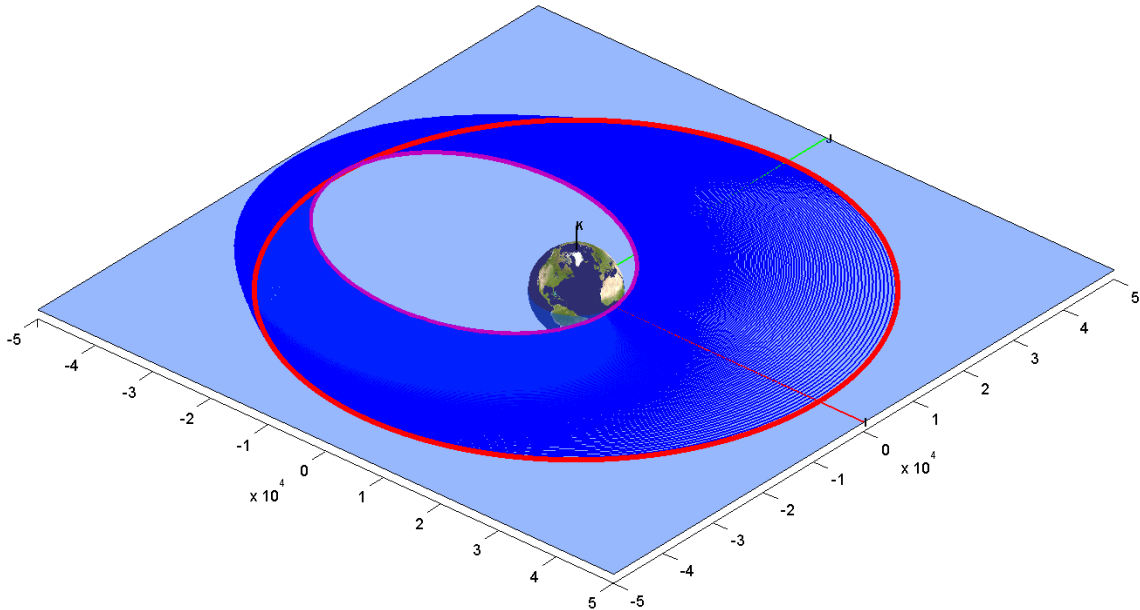


Figure 8. Transfer trajectory from GTO (magenta line) to GEO (red line).

Figure 9 shows the change in time of a , e , and i together with the total maneuver efficiency. Total maneuver efficiency has been defined as the average of the instantaneous maneuver efficiency (see Eq. 14) of each COE.

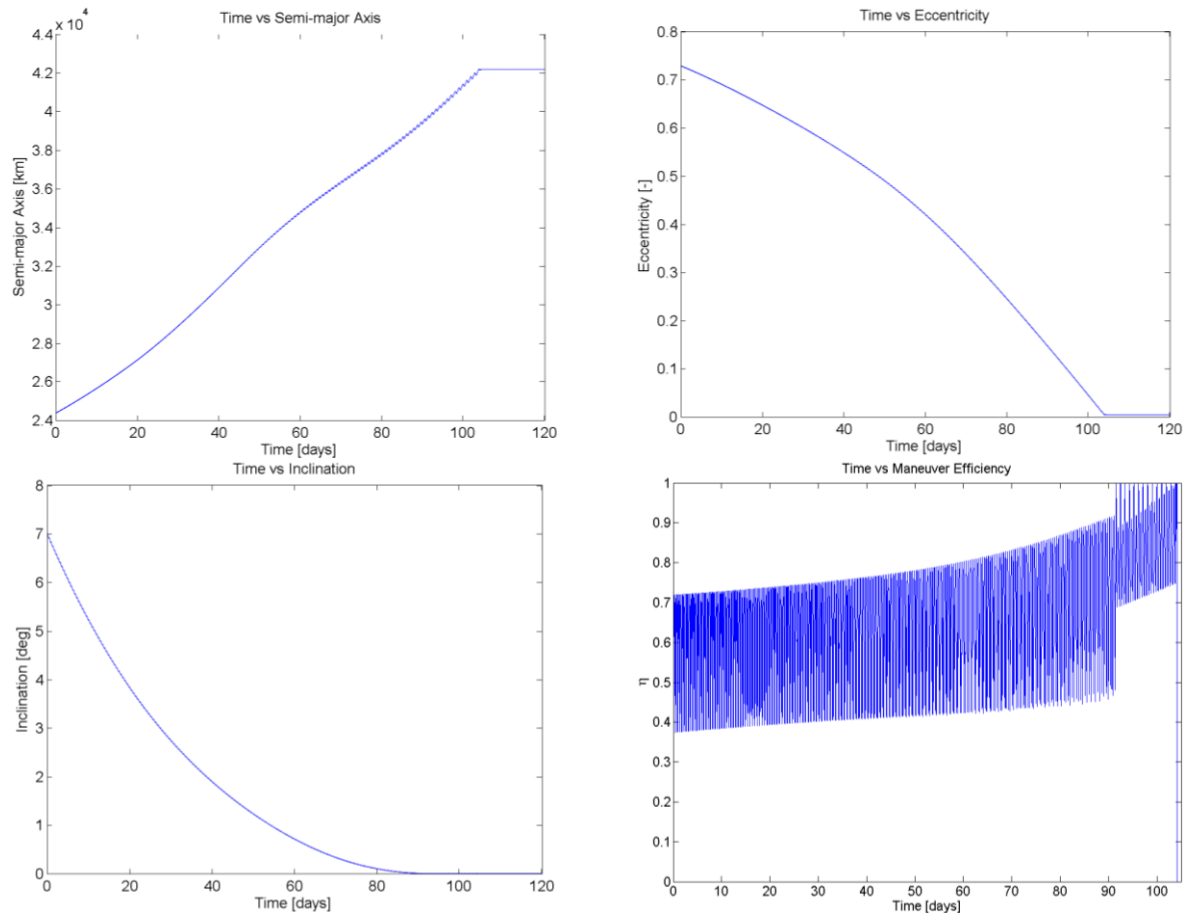


Figure 9. Change in time of a (top left) , e (top right) , i (bottom left) and total maneuver efficiency (bottom right)

The total maneuver efficiency shown in Fig. 9 oscillates, at the beginning of the trajectory, in a small range, reaching the highest possible value (1) only at the end of the transfer. Considering the initial efficiency range (0.4 - 0.7), it is possible to set a maneuver efficiency threshold, as for the inclination change of Fig. 7, to obtain a reduction in the propellant mass consumption and an increase of total transfer time. Figure 10 shows total maneuver time and propellant mass consumption for three different values of maneuver efficiency (left) and the propellant mass consumption for a minimum maneuver efficiency of 70% (right).

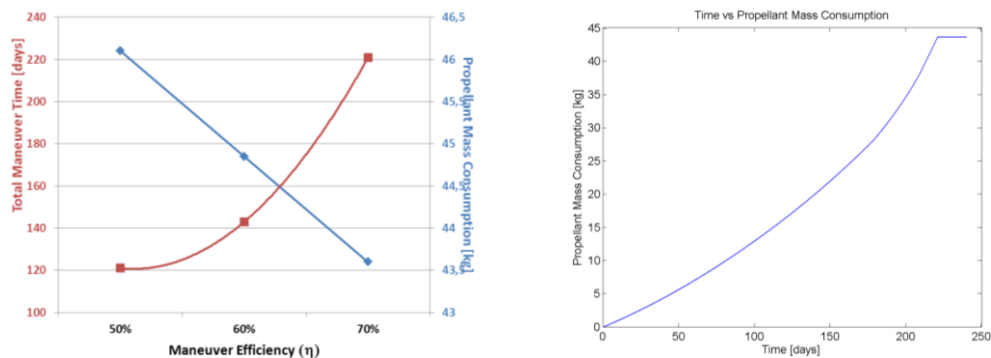


Figure 10. Left: Total maneuver time and propellant mass consumption for different values of maneuver efficiency. Right: Propellant Mass consumption history for a minimum maneuver efficiency of 70%.

From the right plot of Fig. 10 it is possible to notice that mass consumption does not grow uniformly in time and that only at the end of the transfer, when average maneuver efficiency is higher (see Fig. 9), the thruster is operated continuously. It is worth stressing that both in the continuous thrusting case and in case of minimum maneuver efficiency threshold set, the steering program is conceived in such a way that targeted COEs reach their final value at the same time.

V. Conclusion

This study identifies the instantaneous optima in-plane and out-of-plane thrust angles for the modification of classical orbital elements by means of low-thrust maneuvers. Some simplified thrusting laws enabling the modification of one single orbital element with no net effect on the others have been also presented.

For each orbital elements, the identified thrust law have been verified, by means of direct numerical simulation using Alta's proprietary software (SATSLab), and the resulting total velocity increment required to perform such changes compared with analytical approximations available in literature.

A maneuver efficiency has been defined, for each described thrust law, as the ratio between the optimal instantaneous change of a specific COE and the maximum allowable change of the same COE over the orbit. Moreover, it has been demonstrated that, defining a minimum threshold for the maneuver efficiency, a reduction in propellant mass consumption can be obtained with a parallel increase in total maneuver time.

The modification of more than one orbital elements at the same time has been also addressed and obtained. Also in this case, it has been shown that some values of the maneuver efficiency threshold could result in different transfer time and propellant mass consumption.

The outcome of present analysis can be significantly improved both introducing an efficiency threshold value changing during the maneuver and combining the transfer strategy with the effects deriving from orbital perturbation acceleration, i.e. third body acceleration, atmospheric drag, Earth's oblateness, solar radiation pressure.

References

- ¹Polk, J. E., Brinza, D., Kakuda, R. Y., Brophy, J. R., Katz, I., Anderson, J. R., Rawlin, V. K., Patterson, M. J., Sovey, J., Hamley, J., "Demonstration of the NSTAR Ion Propulsion System on the Deep Space One Mission," *27th International Electric Propulsion Conference*, 2001.
- ²Saccoccia, G., Estublier, D., Racca, G. "SMART-1: A Technology Demonstration Mission for Science Using Electric Propulsion," AIAA-98-3330, 34th Joint Propulsion Conference, 1998.
- ³Killinger, R., Kukies, R., Surauer, M., Saccoccia, G., Gray, H., "Final Report on the ARTEMIS Salvage Mission Using Electric Propulsion" 39th Joint Propulsion Conference, Huntsville, AL, 2003, AIAA-2003-4546.
- ⁴Kiforenko, B. N. and Vasil'ev, I. Yu., "On optimization of many-revolution low-thrust orbit transfers: Part 1," *International Applied Mechanics*, Vol. 44, No. 7, pp. 810-817, 2008
- ⁵Garcia Yarnoz, D., Jehn, R., and Croon, M., "Interplanetary Navigation Along the Low-Thrust Trajectory of Bepi Colombo," *Acta Astronautica*, Vol. 59, No. 1-5, pp. 284 – 293, 2006.
- ⁶Spitzer, A., "Novel Orbit Raising Strategy Makes Low Thrust Commercially Viable," *24th International Electric Propulsion Conference*, 1995.
- ⁷Betts, J.T., "Very low-thrust trajectory optimization method using a direct SQP method," *Journal of Computational and Applied Mathematics*, Vol. 120, No. 1-2, pp. 27-40, 2000.
- ⁸Battin, R.H., *An Introduction to the Mathematics and Methods of Astrodynamics*, AIAA Education Series, AIAA, New York, 1987.
- ⁹Vallado, D.A., *Fundamentals of Astrodynamics and Applications*, McGraw-Hill, New York, 1997.
- ¹⁰Marcuccio, S., Ruggiero, A., "Integrated Trajectory and Energy Management Simulator for Electric Propulsion Spacecraft", Proc. 11th Int. Workshop on Simulation & EGSE facilities for Space Programmes, Noordwijk, The Netherlands, 2010
- ¹¹Ruggiero, A., Pergola, P., Marcuccio, S., "Joint Trajectory and Energy Management Simulation of Low Thrust Missions", IEP-11-260, Proc. 32nd International Electric Propulsion Conference, 2011.
- ¹²Edelbaum, T. N., "Propulsion Requirements for Controllable Satellites," *ARS Journal*, Vol. 31, No. 8, pp. 1079-89, 1961.
- ¹³Spitzer A., "Near Optimal Transfer Orbit Trajectory Using Electric Propulsion," *AAS/AIAA Spaceflight Mechanics Conference*, 1995.
- ¹⁴Pollard, J.E., "Simplified Approach for Assessment of Low-Thrust Elliptical Orbit Transfers," *27th International Electric Propulsion Conference*, 2001.
- ¹⁵Petropoulos, A.E., "Simple Control Laws for Low-Thrust Orbit Transfers", AAS/AIAA Astrodynamics Specialists Conference, 2003.
- ¹⁶Pollard, J.E., "Simplified Analysis of Low-Thrust Orbital Maneuvers," Aerospace Report No. TR-2000(8565)-10, 2000.
- ¹⁷Burt, E.G.C., "On Space Manoeuvres with Continuous Thrust," *Planetary and Space Science*, Vol. 15, No. 1, pp. 103-122, 1967.

- ¹⁸Estublier, D., Saccoccia G. and Gonzalez del Amo, J., “Electric Propulsion on SMART-1 - A Technology Milestone,” *ESA Bulletin*, Vol. 129, pp. 40-46, 2007.
- ¹⁹Marchandise, F., Cornu, N., Darnon, F. and Estublier, D., “PPS®1350-G Qualification status 10500 h,” *27th International Electric Propulsion Conference*, 2001.
- ²⁰Gefert, L.P. and Hack, K.J., “Low-Thrust Control Law Development for Transfer from Low Earth Orbits to High Energy Elliptical Parking Orbits,” AAS/AIAA Astrodynamics Specialists Conference, 1999.
- ²¹Falck R. and Gefert L., “A Method of Efficient Inclination Changes for Low-Thrust Spacecraft”, AAS/AIAA Astrodynamics Specialists Conference, 2002.
- ²²Petropoulos, A.E., “Refinements to the Q-law for low-thrust orbit transfers”, AAS/AIAA Astrodynamics Specialists Conference, 2005